4-5-2011

Oxygen Vacancies Adjacent to Cu(2+) Ions in TiO(2) (Rutile) Crystals

A. T. Brant
West Virginia University

Shan Yang (杨山)
West Virginia University

Nancy C. Giles
Air Force Institute of Technology

Zafar Iqbal
COMSATS Institute of Information Technology, Pakistan

A. Manivannan
West Virginia University

See next page for additional authors

Recommended Citation

Brant, A. T., Yang, S., Giles, N. C., Iqbal, M. Z., Manivannan, A., & Halliburton, L. E. (2011). Oxygen vacancies adjacent to Cu 2+ ions in TiO 2 (Rutile) crystals. Journal of Applied Physics, 109(7), 073711. https://doi.org/10.1063/1.3552910

Authors

A. T. Brant, Shan Yang (杨山), Nancy C. Giles, Zafar Iqbal, A. Manivannan, and Larry E. Halliburton

Oxygen vacancies adjacent to Cu²⁺ ions in TiO₂ (rutile) crystals ⊘

A. T. Brant; Shan Yang; N. C. Giles; M. Zafar Iqbal; A. Manivannan; L. E. Halliburton

⊙ Check for updates

CrossMark

⊕ View Online   ↱ Export Citation

Articles You May Be Interested In

Photoinduced trapping of charge at sulfur vacancies and copper ions in photorefractive $Sn_2P_2S_6$ crystals

Journal of Applied Physics (February 2021)

Ground state of the singly ionized oxygen vacancy in rutile TiO_2

Journal of Applied Physics (September 2013)

Time-dependent open-circuit voltage in $CuInSe_2$/CdS solar cells: Theory and experiment

Journal of Applied Physics (May 1987)

Oxygen vacancies adjacent to Cu^{2+} ions in TiO_2 (rutile) crystals

A. T. Brant,[1] Shan Yang (杨山),[1] N. C. Giles,[2] M. Zafar Iqbal,[3] A. Manivannan,[1,4] and L. E. Halliburton[1,a)]

[1]*Department of Physics, West Virginia University, Morgantown, West Virginia 26506, USA*
[2]*Department of Engineering Physics, Air Force Institute of Technology, Wright-Patterson Air Force Base, Ohio 45433, USA*
[3]*Department of Physics, COMSATS Institute of Information Technology, Islamabad 30, Sector H-8/1, Pakistan*
[4]*National Energy Technology Laboratory, Morgantown, West Virginia 26507, USA*

Electron paramagnetic resonance (EPR) and electron-nuclear double resonance (ENDOR) are used to characterize Cu^{2+} ions substituting for Ti^{4+} ions in nominally undoped TiO_2 crystals having the rutile structure. Illumination at 25 K with 442 nm laser light reduces the concentration of Cu^{2+} ions by more than a factor of 2. The laser light also reduces the EPR signals from Fe^{3+} and Cr^{3+} ions and introduces signals from Ti^{3+} ions. Warming in the dark to room temperature restores the crystal to its preilluminated state. Monitoring the recovery of the photoinduced changes in the Cu^{2+} ions and the other paramagnetic electron and hole traps as the temperature is raised from 25 K to room temperature provides evidence that the Cu^{2+} ions have an adjacent doubly ionized oxygen vacancy. These oxygen vacancies serve as charge compensators for the substitutional Cu^{2+} ions and lead to the formation of electrically neutral Cu^{2+}-V_O complexes during growth of the crystals. The Cu^{2+}-V_O complexes act as electron traps and convert to nonparamagnetic Cu^{+}-V_O complexes when the crystals are illuminated at low temperature. Complete sets of spin-Hamiltonian parameters describing the electron Zeeman, hyperfine, and nuclear electric quadrupole interactions for both the ^{63}Cu and ^{65}Cu nuclei are obtained from the EPR and ENDOR data. This study suggests that other divalent cation impurities in TiO_2 such as Co^{2+} and Ni^{2+} may also have an adjacent oxygen vacancy for charge compensation. © *2011 American Institute of Physics*. [doi:10.1063/1.3552910]

I. INTRODUCTION

Room-temperature ferromagnetism in wide-band-gap semiconductors is currently a topic of considerable interest. One material receiving attention is copper-doped titanium dioxide (TiO_2:Cu). The results of *ab initio* calculations[1–5] suggest that an oxygen vacancy immediately adjacent to a substitutional copper ion is necessary to induce ferromagnetism in this material. Until now, there has been limited experimental evidence[6] to support this model for the origin of the ferromagnetism in TiO_2:Cu. Photocatalysis is another important area of interest for TiO_2. Selective doping with anion or cation impurities is used to alter the optical absorption properties of the material and improve the photoresponse. Several research groups[7–10] have investigated the effect of copper doping on the photocatalytic activity of TiO_2.

In the present paper, electron paramagnetic resonance (EPR) and electron-nuclear double resonance (ENDOR) are used to characterize Cu^{2+} ($3d^9$) ions in single crystals of TiO_2 (rutile), with special attention being given to the nuclear electric quadrupole term in the spin Hamiltonian. Gerritsen and Sabisky[11] initially observed the EPR signal from these Cu^{2+} ions and reported approximate values for their **g** and hyperfine matrices. In a more detailed study, Ensign *et al.*[12] obtained parameters describing the electron Zeeman, hyperfine, and

nuclear electric quadrupole interactions. So and Belford,[13] however, commented that the second-order perturbation analysis used by Ensign *et al.*[12] did not provide accurate values for the nuclear electric quadrupole parameters. Improved values for the quadrupole parameters were determined by So and Belford[13] when they used complete diagonalizations of the 8×8 spin-Hamiltonian matrix to reanalyze the original ^{63}Cu data from Ensign *et al.*[12] The present study addresses this lack of a comprehensive set of Cu^{2+} parameters in the literature for TiO_2. We acquire EPR spectra after carefully aligning the magnetic field along the [001], [100], and [110] directions and then perform complete diagonalizations of the spin-Hamiltonian to extract consistent sets of hyperfine parameters for the ^{63}Cu and ^{65}Cu nuclei.

The present paper also addresses the important question of a specific model for the environment surrounding the Cu^{2+} ions in TiO_2 (rutile) crystals. We investigate photoinduced changes in the charge state of these ions and obtain evidence that an oxygen vacancy is adjacent to each Cu^{2+} ion. During an illumination with 442 nm laser light at 25 K, the concentration of Cu^{2+} ions decreases by more than a factor of 2 (this is accompanied by a decrease in the concentration of substitutional Fe^{3+} and Cr^{3+} ions and the appearance of defects containing substitutional Ti^{3+} ions). Warming the crystal to room temperature after removing the laser light provides data indicating that a significant portion of the Cu^{2+} ions trap an electron and convert to Cu^{+} ($3d^{10}$) ions during the illumination at 25 K. Since the Cu^{2+} ions

---

substitute for Ti^{4+} ions (as shown by EPR), this photoinduced behavior is best explained if the copper-related paramagnetic defects initially present in the as-grown crystals are electrically neutral Cu^{2+}-V_O complexes (i.e., close-associate pairs consisting of a Cu^{2+} ion replacing a regular Ti^{4+} ion and an adjacent doubly ionized oxygen vacancy). The only unpaired spin in this Cu^{2+}-V_O complex is localized in a d orbital on the Cu^{2+} ion. In the present paper, we use an ionic notation for the charge states of the transition-metal ions. Results obtained from a TiO_2 (rutile) crystal reduced at high temperature in flowing nitrogen gas support the model of oxygen vacancies adjacent to Cu^{2+} ions.

II. EXPERIMENTAL

The bulk single crystals of TiO_2 (rutile) used in this investigation were obtained from CrysTec (Berlin, Germany) and Nakazumi Crystal Company (Osaka, Japan). Both of these companies used the Verneuil growth technique. Copper was an unintentional impurity in all of our crystals, and similar EPR results were obtained from each crystal. The concentrations of Cu^{2+}, Fe^{3+}, and Cr^{3+} ions in our as-received crystals, as determined with EPR, were in the 1 to 5 ppm range. These estimates are based on comparisons with a calibrated weak-pitch EPR sample provided by Bruker.

A Bruker EMX spectrometer was used to take EPR data and a Bruker Elexsys E-500 spectrometer was used to take ENDOR data. These spectrometers operated near 9.45 GHz. The dimensions of the samples used in the EPR and ENDOR experiments were approximately $1 \times 5 \times 3$ mm^3. Low temperatures were maintained in both spectrometers by using helium-gas flow systems. The optimum temperatures to observe the Cu^{2+} EPR signals, Ti^{3+}-related EPR signals, and Cu^{2+} ENDOR signals were 18, 25, and 15 K, respectively. Magnetic fields were measured with proton NMR gaussmeters. A Cr-doped MgO crystal was used to correct for the difference in magnetic field between the sample and the probe tips of the gaussmeters (the isotropic g value for Cr^{3+} in MgO is 1.9800). During the low-temperature illuminations, approximately 15 mW of 442 nm light from a He-Cd laser was incident on the sample.

III. EPR AND ENDOR RESULTS

The EPR spectra of Cu^{2+} ($3d^9$) ions in TiO_2 (rutile) crystals contain resolved hyperfine lines due to the ^{63}Cu and ^{65}Cu nuclei (69.2 and 30.8% abundant, respectively). Both Cu isotopes have nuclear spin I = 3/2. Compared to the ^{63}Cu nucleus, the ^{65}Cu nucleus has a slightly larger nuclear magnetic moment[14] and a slightly smaller nuclear electric quadrupole moment.[15] Forbidden transitions ($\Delta M_S = \pm 1$, $\Delta m_I = \pm 1$ and $\Delta M_S = \pm 1$, $\Delta m_I = \pm 2$) are present in these EPR spectra along with the usual allowed transitions ($\Delta M_S = \pm 1$, $\Delta m_I = 0$). The Cu^{2+} EPR spectrum taken at 18 K with the magnetic field along the [001] direction is shown in Fig. 1. Figures 2 and 3 show spectra taken at this same temperature when the magnetic field is along the [100] and [110] directions, respectively. Stick diagrams above the spectra in Figs. 1, 2 and 3(a) identify the regions where allowed and forbidden transitions appear (these stick diagrams represent the
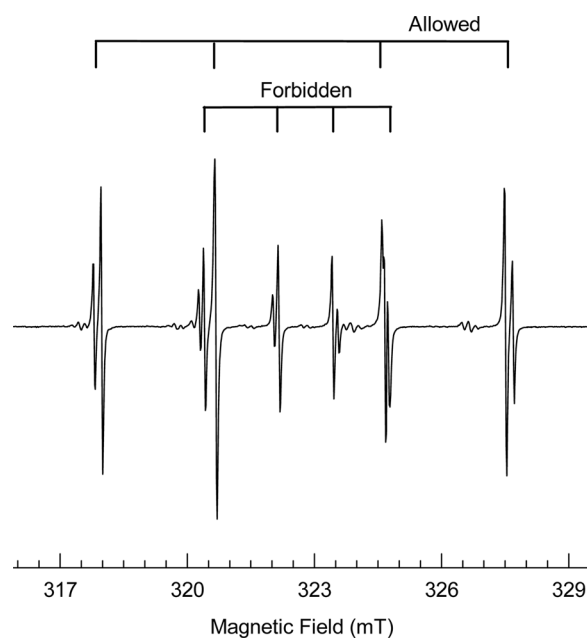

FIG. 1. EPR spectrum of Cu^{2+} ions in a TiO_2 (rutile) crystal. These data were taken at 18 K with the magnetic field along the [001] direction. The microwave frequency was 9.4717 GHz. Stick diagrams illustrate the regions of "allowed" and "forbidden" transitions.

average location of each pair of ^{63}Cu and ^{65}Cu hyperfine lines). The forbidden lines in Figs. 1 and 3(a) are $\Delta m_I = \pm 2$ transitions because the magnetic field is along a principal axis of the hyperfine matrix. In Fig. 2, the magnetic field is not along a principal axis and the forbidden lines are $\Delta m_I = \pm 1$ transitions. In Fig. 3(b), the forbidden lines have essentially zero intensity and are not observed. At 18 K, the experimental EPR linewidths are approximately 0.02 mT. The lines broaden significantly when the temperature increases above 40 K and the EPR signals, although present, become difficult to detect.

FIG. 2. EPR spectrum of Cu^{2+} ions in a TiO_2 (rutile) crystal. These data were taken at 18 K with the magnetic field along the [100] direction. The microwave frequency was 9.4749 GHz. Stick diagrams illustrate the regions of "allowed" and "forbidden" transitions.
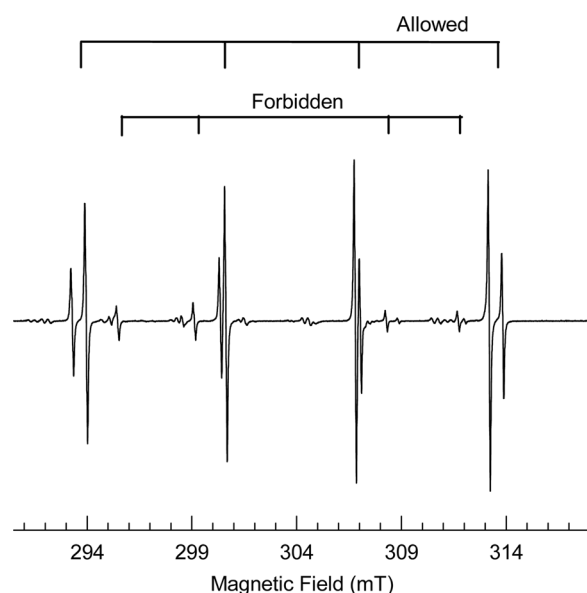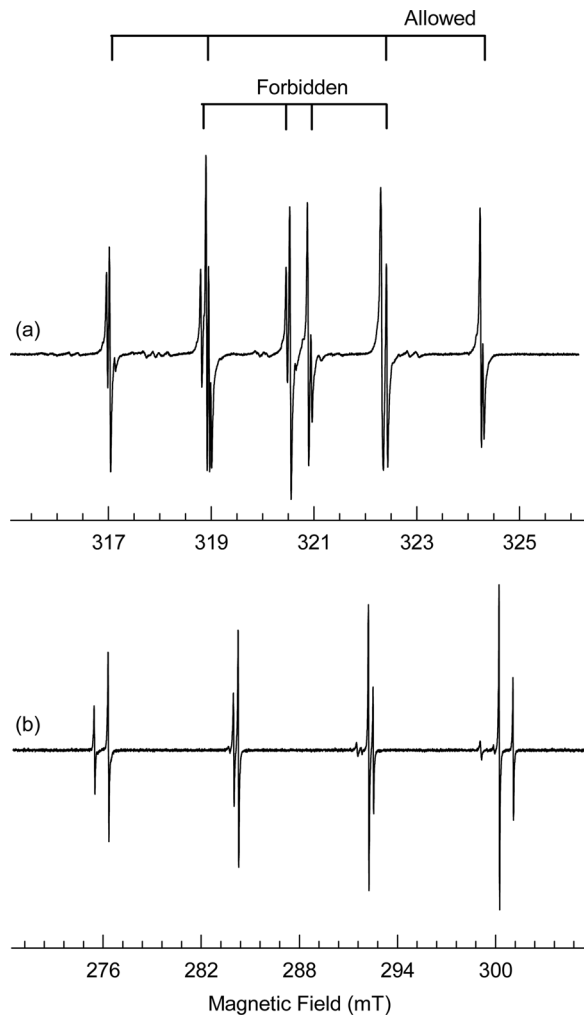
FIG. 3. EPR spectra of Cu^{2+} ions in a TiO_2 (rutile) crystal. These data were taken at 18 K with the magnetic field along the [110] direction. The microwave frequency was 9.4756 GHz. The two crystallographically equivalent, but magnetically inequivalent, sites for this direction of magnetic field give rise to (a) one set of lines at higher field and (b) one set of lines at lower field.

In the TiO_2 (rutile) lattice, there are two equivalent distorted TiO_6 octahedra related by a 90° rotation about the [001] direction. One of these TiO_6 units is illustrated in Fig. 4. The TiO_6 units are elongated in directions perpendicular to the [001] direction with the six oxygen ions separating into a set of two along the elongation directions and a set
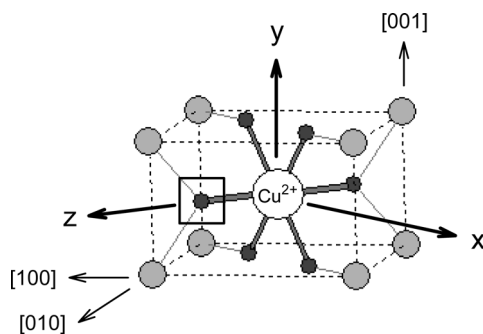

FIG. 4. TiO_2 (rutile) crystal structure showing a TiO_6 unit. A Cu^{2+} ion substitutes for a Ti^{4+} ion and has an oxygen vacancy along the [110] direction. The x, y, and z directions are the principal-axis directions for the **g**, **A**, and **P** matrices.

of four in the (110) planes perpendicular to the elongation directions. Our EPR spectra are consistent with Cu^{2+} ions substituting for Ti^{4+} ions and thus forming two crystallographically equivalent sites that correspond to the two TiO_6 units. All of the Cu^{2+} ions are magnetically equivalent when the magnetic field is along the [001] and [100] directions and one set of EPR lines is observed in each case (see Figs. 1 and 2). There are two crystallographically equivalent, but magnetically inequivalent, sites for the Cu^{2+} ions when the magnetic field is along the [110] direction and two sets of lines are observed (see Fig. 3). The EPR angular dependence of the Cu^{2+} ions shown in Fig. 5 reflects the symmetry of the lattice and requires the directions of the principal axes of the **g** and hyperfine matrices to be along the [$\bar{1}$10], [001], and [110] crystal directions. Specifically, these directions are turning points in the angular-dependence plot. In Fig. 4, these principal-axis directions are labeled x, y, and z. As initially recognized by Ensign *et al.*,[12] having the principal axes of the spin-Hamiltonian matrices along the high-symmetry directions in the crystal is not consistent with the Cu^{2+} ions occupying an interstitial position.

The following spin Hamiltonian is used to analyze the Cu^{2+} EPR and ENDOR spectra:

$$\mathbf{H} = \beta \mathbf{SgB} + \mathbf{IAS} + \mathbf{IPI} - g_N \beta_N \mathbf{IB}. \quad (1)$$

Electron Zeeman, hyperfine, nuclear electric quadrupole, and nuclear Zeeman interactions are included.[16] In the present case, the principal axes of the **g**, **A**, and **P** matrices are collinear and coincide with high symmetry directions in the crystal, thus, Euler angles are not needed to specify these directions. This leaves eight spin-Hamiltonian parameters to describe a Cu^{2+} ion in rutile-structured TiO_2 (three principal values for the **g** matrix, three principal values for the **A** matrix, and two principal values for the **P** matrix). The **P** matrix is traceless and only two principal values must be determined from experiment.

Values of the ^{63}Cu and ^{65}Cu parameters were determined independently. The EPR spectra taken along high-symmetry directions were used to establish the "best" values for the sixteen parameters (eight for ^{63}Cu and eight for ^{65}Cu). Our least-squares fitting procedure involved exact diagonalizations of the 8×8 Hamiltonian matrix (S = 1/2, I = 3/2). For each isotope, the input data consisted of 28 magnetic field values and their associated microwave frequencies. These included four allowed and four forbidden ($\Delta m_I = \pm 2$) lines from the [001] spectrum in Fig. 1, four allowed and four forbidden ($\Delta m_I = \pm 1$) lines from the [100] spectrum in Fig. 2, four allowed and four forbidden ($\Delta m_I = \pm 2$) lines from the [110] high-field spectrum in Fig. 3(a), and four allowed lines from the [110] low-field spectrum in Fig. 3(b). Results from the fitting process are summarized in Table I for each isotope. These best-fit parameters gave an average deviation between predicted and measured magnetic fields of 0.01 mT for the lines used in each fitting. This average deviation is within the measured 0.02 mT linewidths and indicates a good fit to both the allowed and forbidden transitions. As deduced earlier by Ensign *et al.*,[12] the measured **g** matrix is consistent with the unpaired spin (i.e., the unpaired d electron) occupying a d_{xy} orbital on the Cu^{2+} ($3d^9$) ion. This orbital is defined in terms

TABLE I. Spin-Hamiltonian parameters for Cu^{2+} ions in TiO_2 (rutile). The ^{63}Cu and ^{65}Cu values were determined independently. Estimated error limits are ± 0.0001 for the g values, ± 0.3 MHz for the A values, and ± 0.2 MHz for the P values.

	Principal values		
	^{65}Cu	^{63}Cu	Principal-axis directions
g matrix			
g_x	2.10699	2.10697	$[\bar{1}10]$
g_y	2.09281	2.09280	$[001]$
g_z	2.34518	2.34516	$[110]$
Hyperfine matrices			
A_x	+ 55.35 MHz	+ 59.20 MHz	$[\bar{1}10]$
A_y	+ 82.34 MHz	+ 88.21 MHz	$[001]$
A_z	− 261.98 MHz	− 280.83 MHz	$[110]$
Quadrupole matrices			
P_x	− 10.95 MHz	− 10.11 MHz	$[\bar{1}10]$
P_y	− 9.23 MHz	− 8.51 MHz	$[001]$
P_z	+ 20.18 MHz	+18.62 MHz	$[110]$

of the x, y, z coordinate system specified in Fig. 4. The complete angular dependence of the allowed ^{63}Cu EPR lines when the magnetic field is rotated in the $(\bar{1}10)$ and (001) planes is shown in Fig. 5. For ease of viewing, forbidden lines are not plotted in Fig. 5. The discrete points in this figure are experimental data and the solid curves are computer generated using the final set of "best" spin-Hamiltonian parameters.

The absolute signs of the hyperfine and nuclear electric quadrupole parameters in Table I cannot be determined from experiment. Following the original work of Bleaney and co-workers in diluted copper salts,[17–19] we assign a negative sign to A_z and positive signs to A_x and A_y. Experiment does provide the relative signs of the hyperfine and nuclear electric quadrupole parameters. Of the four forbidden ($\Delta m_I = \pm 2$) lin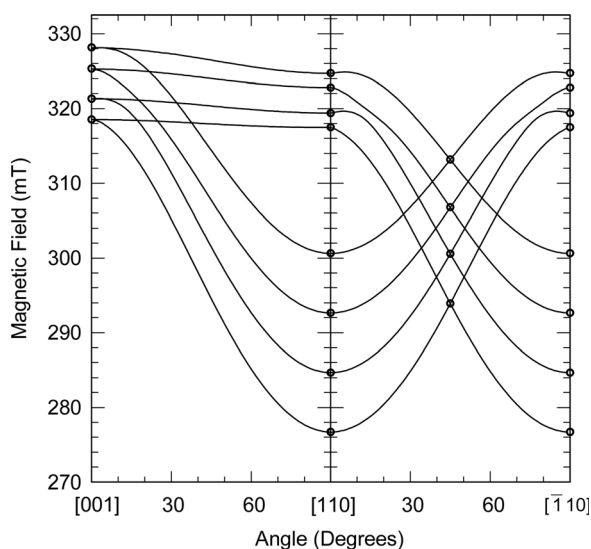es in the [001] spectrum in Fig. 1, the two on the low-field side have a larger separation than the two on the high-field side. This requires P_y and A_y to have opposite signs. Similarly, of the four forbidden ($\Delta m_I = \pm 2$) lines in the [110] spectrum in Fig. 3(a), the two on the low-field side have a larger separation than the two on the high-field side. This requires P_x and A_x to have opposite signs. Thus, P_x and P_y must have negative signs, given our assignment of positive signs to A_x and A_y. Since the quadrupole matrix is traceless, P_z must have a positive sign (opposite to that of P_x and P_y).

Figures 6 and 7 show ^{63}Cu ENDOR spectra from the Cu^{2+} ions in TiO_2 (rutile). These data provide an independent check of the values of the parameters listed in Table I (especially the nuclear electric quadrupole parameters). The ENDOR spectra in Fig. 6 were taken at 15 K with a microwave frequency of 9.40355 GHz and the magnetic field along the [001] direction. The spectra in trace (a) and trace (b) were obtained from the lowest-field and highest-field ^{63}Cu EPR lines in Fig. 1, respectively. As usual, the ENDOR lines appear in pairs. Dominant ENDOR lines occur at 14.54 and 66.23 MHz in trace (a), while the exact-diagonalization predictions using the parameters in Table I place the lines at 14.70 and 66.54 MHz. Similarly, the dominant lines in trace (b) occur at 22.70 and 61.35 MHz and the exact-diagonalization predictions are 22.23 and 61.12 MHz. The differences between the measured and predicted values of line positions are less than the linewidth in both traces. The widths of the ENDOR lines in Fig. 6 are large, varying from 740 to 830 kHz, and are a result of the large nuclear electric quadrupole interaction.

Figure 7 shows ^{63}Cu ENDOR data taken at 15 K with a microwave frequency of 9.42953 GHz and the magnetic field along the [100] direction. Here the signals in trace (a) and trace (b) were obtained from the lowest-field and highest-field ^{63}Cu EPR lines in Fig. 2, respectively. The upper radio frequency limit of the spectrometer prevented the observation of the second ENDOR line in each of these spectra. In trace (a), the line occurs at 47.17 MHz and the predicted position is
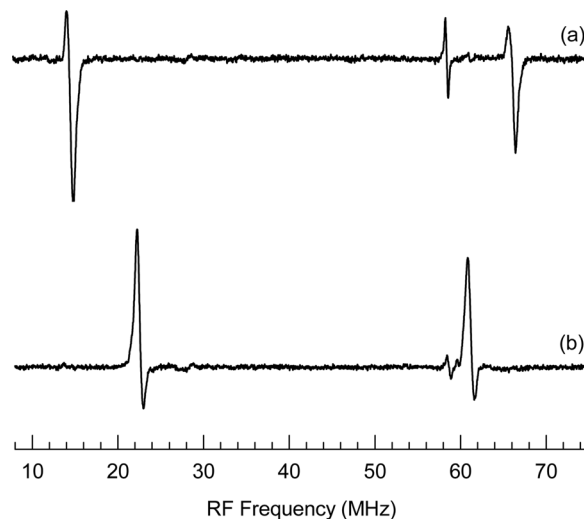

FIG. 5. EPR angular dependence of Cu^{2+} ions in a TiO_2 (rutile) crystal. The microwave frequency is 9.4747 GHz. For simplicity, only the "allowed" transitions for ^{63}Cu are plotted for rotations in the $(\bar{1}10)$ and (001) planes. There are two equivalent sites occupied by the Cu^{2+} ions. The solid curves are computer-generated using the ^{63}Cu parameters listed in Table I. The discrete points are experimental data.

FIG. 6. ENDOR spectra of ^{63}Cu nuclei in a TiO_2 (rutile) crystal. These data were taken at 15 K with the magnetic field along the [001] direction. (a) The magnetic field was set at 316.146 mT, which in the ENDOR cavity corresponded to the lowest-field allowed line in the EPR spectrum in Fig. 1. (b) The magnetic field was set at 325.707 mT, corresponding to the highest-field allowed line in the EPR spectrum in Fig. 1.
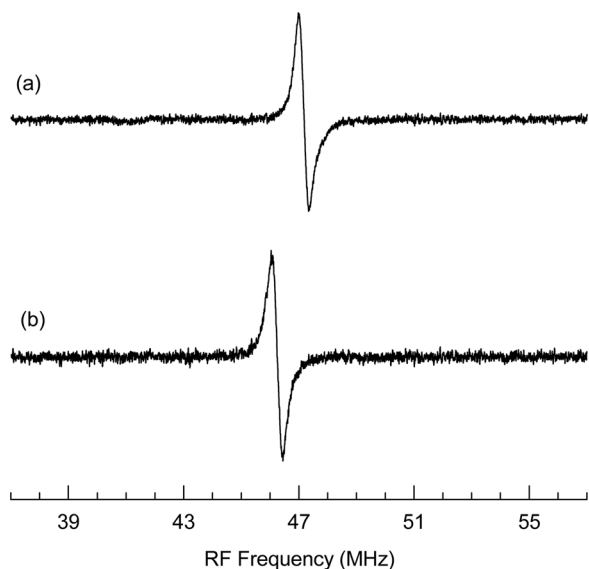
FIG. 7. ENDOR spectra of ^{63}Cu nuclei in a TiO_2 (rutile) crystal. These data were taken at 15 K with the magnetic field along the [100] direction. (a) The magnetic field was set at 292.455 mT, which in the ENDOR cavity corresponded to the lowest-field allowed line in the EPR spectrum in Fig. 2. (b) The magnetic field was set at 311.775 mT, corresponding to the highest-field allowed line in the EPR spectrum in Fig. 2.

46.83 MHz. For the line in trace (b), the experimental position is 46.25 MHz and the predicted position is 45.88 MHz.

From Table I, the ratios of the principal hyperfine values for the two isotopes (i.e., $^{65}A_i/^{63}A_i$ where i = x, y, z) are 1.070, 1.071, and 1.072, which agrees with the known values[14] of the nuclear g factors (1.588 for ^{65}Cu and 1.484 for ^{63}Cu). Similarly, the ratios of the principal quadrupole values for the two isotopes (i.e., $^{65}P_i/^{63}P_i$) in Table I are 0.923, 0.922, and 0.923, which agrees with the earlier ratio determination of $^{65}Q/^{63}Q = 0.9268$ by Minier and Minier.[20] The presently accepted values[15] of the ^{65}Cu and ^{63}Cu nuclear electric quadrupole moments are -0.204×10^{-28} m^2 and -0.220×10^{-28} m^2, respectively. As predicted by So and Belford,[13] the nuclear electric quadrupole parameters determined in the present study and listed in Table I are significantly different from those initially proposed by Ensign *et al.*[12] Our quadrupole values in Table I are consistently larger in magnitude than those of Ensign *et al.*,[12] with the increases varying from 22 to 44%. Another significant difference is in the values of the A_x hyperfine parameters. Ensign *et al.*[12] have 1.005 for the ratio of $^{65}A_x/^{63}A_x$ whereas we have 1.070 (our value is much closer to the ratio of the known nuclear g factors). Also, our estimated error limits in Table I for the g and A values are smaller than those of Ensign *et al.*[12] The improvements in the values of the spin-Hamiltonian parameters in our study are a result of exact diagonalizations of the Hamiltonian matrix, in contrast to the previously used perturbation theory approach. The present study provides much more accurate values of the electric field gradient that can be used to verify the model of the Cu^{2+} defects in TiO_2 (rutile) crystals (see Sec. VI).

IV. PHOTOINDUCED CHANGES IN CHARGE STATES

Photoexcitation experiments demonstrate that another charge state of copper can exist in our TiO_2 (rutile) crystals.

The three spectra in Fig. 8 were taken at 25 K with the magnetic field along the [001] direction. Spectrometer gain and modulation amplitude settings were the same for each spectrum. Figure 8(a) was taken before exposure to the 442 nm laser light and shows only the EPR spectrum from the Cu^{2+} ions (signals from substitutional Fe^{3+} and Cr^{3+} ions[21–24] were also present). In Fig. 8(b), the laser light reduces the Cu^{2+} signals by more than a factor of 2 and produces three additional spectra. These three lines at 347.8, 353.1, and 375.2 mT are shallow donors previously reported by Yang *et al.*[24] and are assigned to neutral oxygen vacancies (V_O^0), $Ti^{3+}-Si^{4+}$ centers, and singly ionized oxygen vacancies (V_O^+), respectively. Figure 8(c) shows that warming the crystal to 60 K for 1 min after removing the laser light thermally destroys these three additional spectra but does not affect the intensity of the Cu^{2+} spectrum. The EPR signals from the Fe^{3+} and Cr^{3+} ions decrease when the crystal is illuminated at 25 K. These ions serve as deep acceptors (i.e., hole traps) and a portion of them convert to Fe^{4+} and Cr^{4+} ions during the low-temperature illumination. After removing the laser light, the Fe^{3+} and Cr^{3+} signals have a partial recovery step when the crystal is warmed to 60 K (this coincides with the complete disappearance of the three shallow-donor signals). Continued warming of the crystal shows that the Fe^{3+} and Cr^{3+} signals have a
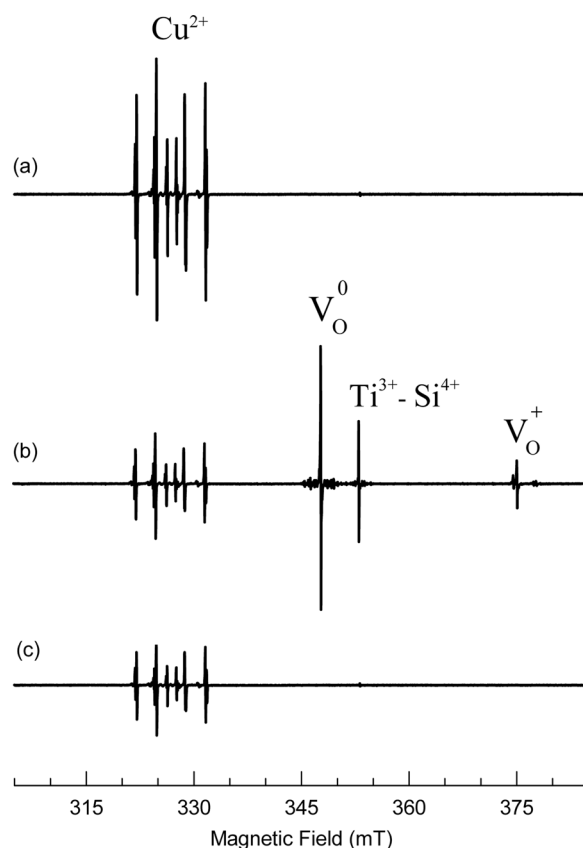

FIG. 8. Photoinduced changes and subsequent annealing behavior of electron and hole traps in a TiO_2 (rutile) crystal. These EPR spectra were taken at 25 K with the magnetic field along the [001] direction. (a) Before illumination. (b) After illumination with 442 nm laser light. (c) After warming the crystal to 60 K in the dark for 1 min and then returning to the lower monitoring temperature.

second broad and final recovery step in the 100 to 200 K region. This second increase in the Fe^{3+} and Cr^{3+} signals coincides with the full recovery of the Cu^{2+} signals.

The earlier work of Yang *et al.*[24] has verified that the neutral oxygen vacancies (V_O^0), the Ti^{3+}-Si^{4+} centers, and the singly ionized oxygen vacancies (V_O^+) present in Fig. 8(b) are electron traps. These three centers have Ti^{3+} ions as their primary component. Photoinduced electrons from substitutional Fe^{3+} and Cr^{3+} impurities are temporarily trapped at these three centers as long as the sample temperature remains near or below 25 K. The question raised by the data in Fig. 8(b) is whether the portion of the Cu^{2+} ions that disappear as a result of the illumination are converted to Cu^+ ions or to Cu^{3+} ions. (In other words, does the observed Cu^{2+} defect act as an electron trap or a hole trap at low temperature in TiO_2?). The answer is found in the data in Fig. 8(c) where warming the crystal to 60 K releases the trapped electrons from the three shallow Ti^{3+}-related centers but does not change the concentration of Cu^{2+} ions. Electrons released from the Ti^{3+}-related centers during the warming to 60 K would recombine with any Cu^{3+} ions (i.e., trapped holes) that are present and increase the concentration of Cu^{2+} ions. On the other hand, thermally released electrons would not recombine with any Cu^+ ions (i.e., trapped electrons) that are present and thus would leave the concentration of Cu^{2+} ions unchanged during the warming to 60 K. The second scenario agrees with the experimental data. Our results in Fig. 8 show that the Cu^{2+} ions in TiO_2 are electron traps (i.e., a portion of the Cu^{2+} ions are converted to Cu^+ ions during an illumination at 25 K with laser light). This conclusion is also supported by our thermal anneal showing that the recovery of the Cu^{2+} ions, following an illumination with laser light at 25 K, occurs in the same temperature range as the second recovery step of the Fe^{3+} and Cr^{3+} ions.

V. REDUCTION EFFECTS

A reduction experiment was performed on one of our TiO_2 crystals. A large Cu^{2+} EPR spectrum was observed at 18 K before the reduction treatment. The crystal was then placed in flowing nitrogen gas and held at 600 °C for 10 min. There was no observable Cu^{2+} EPR signal after the reduction at high temperature. The reduction treatment increases the electrical conductivity of the crystal (i.e., isolated oxygen vacancies introduced during the reduction increase the number of electrons in shallow donor states and in the conduction band). In the reduced crystal, each Cu^{2+} ion traps one of these electrons and converts to a nonparamagnetic Cu^+ ($3d^{10}$) ion. This eliminates the Cu^{2+} EPR signal. Annealing the reduced crystal at 700 °C in air for 30 min removes the reduction effects and restores the crystal to its as-received state. During this oxidation process, oxygen ions diffuse back into the crystal and remove the isolated oxygen vacancies (i.e., shallow donors) that provide the extra electrons, thus allowing the Cu^+ ions to return to Cu^{2+} ions. In other words, the Fermi level is raised by the reduction and lowered by the oxidation. The results of the reduction experiment provide additional evidence that the observed Cu^{2+} ions are electron traps in TiO_2 (rutile) crystals.

VI. DISCUSSION

The principal axes of the spin-Hamiltonian matrices (**g**, **A**, and **P**) for the Cu^{2+} ions coincide with high symmetry directions in the TiO_2 (rutile) lattice, thus establishing that the Cu^{2+} ions substitute for Ti^{4+} ions. Photoinduced and reducing experiments show that these Cu^{2+} ions can act as electron traps (i.e., they convert to Cu^+ ions when "free" or excess electrons are present). Together, these observations allow us to conclude that the Cu^{2+} ions have an adjacent doubly ionized oxygen vacancy. It is unlikely that isolated substitutional Cu^+ ions can exist in the TiO_2 lattice since this would be a defect that deviates (in an ionic view) by three units of charge from the Ti^{4+} ion being replaced and would correspond to a large formation energy. Instead, our data support the formation of electrically neutral Cu^{2+}-V_O complexes in the crystal during growth. Significant concentrations of doubly ionized oxygen vacancies easily form in TiO_2 (rutile) crystals during growth[24] and their association with substitutional Cu^{2+} ions is energetically favorable. With effective charges of 2+ and 2−, a doubly ionized oxygen vacancy and a substitutional Cu^{2+} ion have a strong electrostatic attraction and migrate toward each other to form the electrically neutral Cu^{2+}-V_O complexes (i.e., close-associate pairs) as the crystal cools from the high growth temperature. During the illumination with laser light at low temperature or during the reducing treatment at 600 °C, the paramagnetic Cu^{2+}-V_O defects convert to nonparamagnetic Cu^+-V_O defects. To be consistent with the experimentally determined principal-axis directions of the **g** and hyperfine matrices, the oxygen vacancy must be located at one of the two neighboring oxygen sites in the set of two along the elongation direction of the TiO_6 unit (as shown in Fig. 4).

The spin-Hamiltonian parameters describing the electric quadrupole interactions at the ^{63}Cu and ^{65}Cu nuclei provide a second approach to establish the ground state model of the defect responsible for the Cu^{2+} EPR signal (i.e., to verify that the Cu^{2+} ions have an adjacent doubly ionized oxygen vacancy). Our Cu^{2+} EPR data and their subsequent analysis have resulted in reliable values of the parameters describing the nuclear electric quadrupole interactions. These values, in turn, could be compared to predictions resulting from first-principles calculations of the electric field gradient at the Cu nucleus. As an example of this approach, Blaha *et al.*[25] calculated the electric field gradient at the Ti site in TiO_2 crystals and found good agreement with the experimental results of Kanert and Kolem.[26] Also, the electric field gradients at ^{111}Cd and ^{181}Ta impurities in TiO_2 have been investigated by Errico *et al.*[27] and Darriba *et al.*,[28] respectively. In the present case, our experimental results in Table I could be compared with the results of first-principles calculations of the electric field gradient at the Cu^{2+} nucleus, with and without the adjacent doubly ionized oxygen vacancy. This would provide evidence for or against the presence of the oxygen vacancy adjacent to the Cu^{2+} ion. These first-principles calculations of the electric field gradient at the Cu nucleus, however, must await other investigators as they are beyond the scope of this paper.

The present study demonstrates the dual role of oxygen vacancies in TiO_2 (rutile) crystals. An isolated oxygen

vacancy is a shallow donor with its neutral and singly ionized charge states located near the conduction band.[24] The neutral $(S = 1)$ and the singly ionized $(S = 1/2)$ states of the isolated oxygen vacancy can both be monitored at low temperature with EPR, as shown in Fig. 8. In contrast, the complex consisting of an oxygen vacancy and an adjacent substitutional copper ion acts as an acceptor. In the absence of optical excitation, the complex is in its neutral charge state $(Cu^{2+}-V_O)$ when the Fermi level is low (this is the case for our as-received crystals). When the sample is reduced and the Fermi level moves higher, the complex accepts an electron and changes to its singly ionized charge state (Cu^+-V_O). When doping TiO_2 crystals with other divalent cations such as Co^{2+} or Ni^{2+}, a similar scenario is expected (i.e., an adjacent oxygen vacancy provides charge compensation for the divalent ion and the resulting complex behaves as an acceptor).

VII. SUMMARY

A series of EPR and ENDOR experiments have been performed on Cu^{2+} ions in bulk single crystals of TiO_2 (rutile) and a complete set of spin-Hamiltonian parameters have been determined (see Table I). These parameters are a significant improvement over the earlier set obtained by Ensign *et al.*[12] The important question of the local environment of the Cu^{2+} ions has also been addressed. Photoexcitation experiments at low temperature and reducing experiments at high temperature show that electrically neutral $Cu^{2+}-V_O$ complexes are formed during growth of the TiO_2 crystals. These $Cu^{2+}-V_O$ complexes, consisting of a Cu^{2+} ion replacing a Ti^{4+} ion and an adjacent doubly ionized oxygen vacancy, serve as electron traps and convert to nonparamagnetic Cu^+-V_O complexes when exposed to laser light while at low temperature. A similar conversion occurs when excess electrons are present as a result of a reducing treatment. The angular dependence of the EPR spectra shows that the vacancy occupies one of the two sites in the set of two equivalent neighboring oxygen sites along the elongation direction in a TiO_6 unit (i.e., the oxygen vacancy is located in a [110] or [$\bar{1}$10] direction relative to the substitutional Cu^{2+} ion).

ACKNOWLEDGMENTS

[1]S. Duhalde, M. F. Vignolo, F. Golmar, C. Chiliotte, C. E. Rodriguez Torres, L. A. Errico, A. F. Cabrera, M. Renteria, F. H. Sanchez, and M. Weissmann, Phys. Rev. B **72**, 161313(R) (2005).

[2]L. A. Errico, M. Renteria, and M. Weissmann, Phys. Rev. B **72**, 184425 (2005).

[3]Deng Lu Hou, Rui Bin Zhao, Hai Juan Meng, Li Yun Jia, Xiao Juan Ye, Hong Juan Zhou, and Xiu Ling Li, Thin Solid Films **516**, 3223 (2008).

[4]Q. K. Li, B. Wang, C. H. Woo, H. Wang, Z. Y. Zhu, and R. Wang, Europhys. Lett. **81**, 17004 (2008).

[5]Dongyoo Kim, Jisang Hong, Young Ran Park, and Kwang Joo Kim, J. Phys.: Condens. Matter **21**, 195405 (2009).

[6]M. You, T. G. Kim, and Y. M. Sung, Cryst. Growth Des. **10**, 983 (2010).

[7]G. Colon, M. Maicu, M. C. Hildalgo, and J. A. Navio, Appl. Catal., B **67**, 41 (2006).

[8]X. H. Xia, Y. Gao, Z. Wang, and Z. J. Jia, J. Phys. Chem. Solids **69**, 2888 (2008).

[9]Jina Choi, Hyunwoong Park, and Michael R. Hoffmann, J. Phys. Chem. C **114**, 783 (2010).

[10]Gonghu Li, Nada M. Dimitrijevic, Le Chen, Tijana Rajh, and Kimberly A. Gray, J. Phys. Chem. C **112**, 19040 (2008).

[11]H. J. Gerritsen and E. S. Sabisky, Phys. Rev. **125**, 1853 (1962).

[12]T. C. Ensign, Te-Tse Chang, and A. H. Kahn, Phys. Rev. **188**, 703 (1969).

[13]H. So and R. Linn Belford, Phys. Rev. B **2**, 3810 (1970).

[14]J. A. Weil and J. R. Bolton, *Electron Paramagnetic Resonance: Elementary Theory and Practical Applications,* 2nd ed. (Wiley, New York, 2007), p. 581.

[15]P. Pyykko, Mol. Phys. **106**, 1965 (2008).

[16]J.-M. Spaeth and H. Overhof, *Point Defects in Semiconductors and Insulators: Determination of Atomic and Electronic Structure from Paramagnetic Hyperfine Interactions* (Springer-Verlag, Heidelberg, 2003).

[17]B. Bleaney, K. D. Bowers, and D. J. E. Ingram, Proc. R. Soc. London **A228**, 147 (1955).

[18]B. Bleaney, K. D. Bowers, and R. S. Trenam, Proc. R. Soc. London **A228**, 157 (1955).

[19]B. Bleaney, K. D. Bowers, and M. H. L. Pryce, Proc. R. Soc. London **A228**, 166 (1955).

[20]M. Minier and C. Minier, Phys. Rev. B **22**, 21 (1980).

[21]H. J. Gerritsen, S. E. Harrison, H. R. Lewis, and J. P. Wittke, Phys. Rev. Lett. **2**, 153 (1959).

[22]D. L. Carter and A. Okaya, Phys. Rev. **118**, 1485 (1960).

[23]G. J. Lichtenberger and J. R. Addison, Phys. Rev. **184**, 381 (1969).

[24]S. Yang, L. E. Halliburton, A. Manivannan, P. H. Bunton, D. B. Baker, M. Klemm, S. Horn, and A. Fujishima, Appl. Phys. Lett. **94**, 162114 (2009).

[25]P. Blaha, D. J. Singh, P. I. Sorantin, and K. Schwarz, Phys. Rev. B **46**, 1321 (1992).

[26]O. Kanert and H. Kolem, J. Phys. C **21**, 3909 (1988).

[27]L. A. Errico, G. Fabricius, M. Renteria, P. de la Presa, and M. Forker, Phys. Rev. Lett. **89**, 055503 (2002).

[28]G. N. Darriba, L. A. Errico, P. D. Eversheim, G. Fabricius, and M. Renteria, Phys. Rev. B **79**, 115213 (2009).